

Article

Basic Research on Selective Extraction of Iron from Titanium Dioxide Waste Acid to Prepare Iron Phosphate Precursors

Xuejiao Cao ^{1,*}, Yang Chen ¹, Xinxing Liang ², Yibing Li ¹, Weiguang Zhang ¹, Zhenlei Cai ³ and Ting'an Zhang ⁴

¹ School of Materials Science and Engineering, Guilin University of Technology, Guilin 541004, China; chenyang2313@glut.edu.cn (Y.C.); lybgems@glut.edu.cn (Y.L.); zhangwg@glut.edu.cn (W.Z.)

² Norin Mining Limited, Beijing 100053, China; lxx@norinmining.com

³ National Key Laboratory of Mineral and Metallurgical Resource Utilization and Pollution Control for Environmental Protection, Wuhan University of Science and Technology, Wuhan 430081, China; caizhenlei@wust.edu.cn

⁴ School of Metallurgy, Northeastern University, Shenyang 110819, China; zta2000@163.net

* Correspondence: xuejiaocao@glut.edu.cn; Tel.: +86-15676337372

Abstract: In view of the current situation wherein acid resources and valuable components in titanium dioxide waste acid cannot be effectively extracted and are prone to secondary pollution, our research team proposed a new technique consisting of step extraction and the comprehensive utilization of titanium dioxide waste acid. In this paper, the thermodynamics of selective precipitation and the preparation of doped iron phosphate from waste acid were studied. The thermodynamics results show that the content of Al^{3+} , Mn^{2+} , Mg^{2+} , and Ca^{2+} in the reaction system can be tuned by adjusting the pH during the pre-precipitation process. In the first step, these impurity ions should be settled as much as possible; then, Fe^{2+} should be oxidized to Fe^{3+} so as to obtain iron phosphate with higher purity in the next step of the precipitation process. The effects of the reaction temperature, seed crystals, pH value, and P/M on the precipitation process were investigated in detail. The experimental results show that in the reduced state, the optimal precipitation conditions are a temperature of 75 °C, an initial pH value of 4.5, and an optimal P/M molar ratio of 1.1. In the oxidized state, the optimal precipitation conditions are a temperature of 60 °C, a solution pH = 2.5, and a reaction time of 25 min. After calcination, the precipitate mainly consists of iron phosphate, which basically meets the requirements of an iron phosphate precursor.

Keywords: titanium dioxide waste acid; iron phosphate; precursor; selective extraction



Citation: Cao, X.; Chen, Y.; Liang, X.; Li, Y.; Zhang, W.; Cai, Z.; Zhang, T. Basic Research on Selective Extraction of Iron from Titanium Dioxide Waste Acid to Prepare Iron Phosphate Precursors. *Separations* **2023**, *10*, 400. <https://doi.org/10.3390/separations10070400>

Academic Editor: Marek Majdan

Received: 22 April 2023

Revised: 19 June 2023

Accepted: 26 June 2023

Published: 11 July 2023



Copyright: © 2023 by the authors. Licensee MDPI, Basel, Switzerland. This article is an open access article distributed under the terms and conditions of the Creative Commons Attribution (CC BY) license (<https://creativecommons.org/licenses/by/4.0/>).

1. Introduction

As an important chemical raw material, titanium dioxide offers high chemical stability, heat resistance, weather resistance, good whiteness, and coloring and covering capacity [1]. It is an important white pigment, which is widely used in coating, ceramics, paper-making, rubber manufacturing, and other industries. Its main production methods are the sulfuric acid method and the chlorination method. In China, about 95% of titanium dioxide powder is produced using the sulfuric acid method.

For every 1 t of titanium dioxide produced using the sulfuric acid method, about 8 t of waste sulfuric acid is produced, which contains about 20% acid, about 10% ferrous sulfate, and a small amount of metatitanic acid, magnesium sulfate, aluminum sulfate, manganese sulfate, and other impurities. At present, about 22~26% of titanium dioxide waste acid can be directly reused in the acidolysis process of titanium dioxide production. If the remaining part is discharged directly, it will not only waste resources but also pollute the environment [2–4]. Therefore, the treatment of waste acid directly restricts the survival and development of titanium dioxide production via the sulfuric acid method.

The main treatment methods for titanium dioxide waste acid are the vacuum concentration method and the lime neutralization method [5,6].

At present, the concentration method has been used to treat the waste acid of titanium dioxide by titanium dioxide enterprises in Panxi. In this process, approximately 20% waste sulfuric acid is concentrated into 70% industrial sulfuric acid through a concentration device so as to realize comprehensive utilization. However, the operation effect of the vacuum concentration method when used by titanium dioxide enterprises is not ideal; this is mainly reflected in the following aspects: it is a complex process, it has high operation costs and equipment maintenance costs, and it generates large emissions of the “three wastes”. Accordingly, high equipment investment and operating costs have placed a great deal of pressure on enterprises.

When using the lime neutralization method to treat waste acid, 0.3~0.5 tons of lime is consumed for each ton of waste acid treated, which not only consumes a lot of lime resources but also produces a lot of gypsum slag. At present, these gypsum dregs cannot be effectively used and can only be stacked in slag yards, which not only occupies land resources but also leads to the loss of sulfur resources. Therefore, the lime neutralization method is not in line with the current environmental protection management requirements.

Based on the treatment status of titanium dioxide waste acid, in order to make better use of valuable metal resources and the acid resources in titanium dioxide waste acid, our research team innovatively proposed a new process of “cascade extraction of valuable components from titanium dioxide waste acid”, for which we have applied for several invention patents [7–12]. Firstly, scandium was effectively extracted from waste acid using the solvent extraction method. Secondly, iron from waste acid was prepared into an iron phosphate precursor of lithium iron phosphate for a battery via the selective precipitation method. Finally, vanadium residue was leached by using the acid resources in waste acid.

With regard to the process of developing new energy, lithium-ion batteries, as a new generation of clean and environmentally friendly energy sources, are receiving increasing attention. For lithium-ion batteries, positive and negative electrode materials are the key factors determining their electrochemical performance, safety performance, and cost. In the positive electrode materials of lithium batteries, the advantages of lithium iron phosphate over the traditional positive electrode materials LiCoO_2 and LiMn_2O_4 lie in its cheaper raw materials that can be more widely sourced and the fact that it does not pollute the environment. Moreover, LiFePO_4 has the capacity for reversible lithium intercalation and removal, with a calculated theoretical specific capacity of 170 mA·h/g. It also offers stable electrochemical performance, good cycling performance, and other advantages, and it is widely considered the preferred positive electrode material for lithium-ion batteries. The performance of lithium iron phosphate largely depends on its precursor. Currently, the precursors used to prepare this material are mostly chemically pure or analytically pure iron salts. Most of these high-purity iron salts are obtained from ores through a series of impurity removal processes. Therefore, directly utilizing waste to prepare precursor materials for lithium-ion battery electrodes is an effective method to reduce production costs [13–15].

In recent years, lithium iron phosphate, the cathode material of lithium-ion batteries, has become one of the most promising cathode materials for lithium-ion batteries due to its advantages of high theoretical specific capacity (170 mA·h/g), good cycling performance, good thermal stability, low price, and environmental friendliness [16,17]. At present, most of the iron sources for the preparation of lithium iron phosphate are analytical pure iron salts, mainly including ferrous oxalate, ferrous acetate, ferrous sulfate, iron sulfate, iron nitrate, iron phosphate, iron oxide, etc. The price of these analytical pure iron salts is relatively high, and some doping elements (such as Mg, Mn, Al, Ti, etc.) that are beneficial to these salts' electrochemical properties need to be added when they are used to prepare high-performance lithium iron phosphate [18,19]. These doping elements happen to exist in titanium dioxide waste acid. Therefore, the preparation of the precursor of lithium iron phosphate from titanium dioxide waste acid is a good choice for both the raw material of lithium iron phosphate and the comprehensive utilization of titanium dioxide waste acid. As the precursor of lithium phosphate for batteries, the requirements of iron phosphate are mainly based on the chemical industry standards of the People's Republic of China

(Hg/T 4701-2014) (<<iron phosphate for batter>>) [20–24]. The technical requirements of the standard are as follows: Fe, w/% = 29.0~30.0; P, w/% = 16.2~17.2; molar ratio of Fe:P = 0.97~1.02; and D50/mm = 2~6.

However, in previous research, the optimal conditions for one-step precipitation were reported to be a temperature of 60 °C, an initial pH value of 2.5, an optimal P/Fe molar ratio of 1.1, and a volume of the dispersant polyethylene glycol equal to 5 mL (Per 50 mL of waste acid). However, in this case, the product was doped with a small amount of aluminum phosphate [25]. Therefore, the precipitate mainly consisted of iron phosphate and a small amount of aluminum phosphate, thus failing to meet the requirements of an iron phosphate precursor.

Therefore, a two-step process, namely, the “Pre-removal of impurities in reducing state and iron precipitation in oxidation state”, for preparing iron phosphate from titanium dioxide waste acid was proposed. In other words, when iron is in a reduced state, other impurities can form phosphate and be removed. Then, iron is oxidized to its trivalent state to enable selective precipitation and thus form iron phosphate. This paper focuses on the thermodynamics and the judgment of the suitability (through experimentation) of pre-impurity removal in the reduced state and the influence of temperature, seed addition, pH value, and P/Me on the subsequent precipitation of iron phosphate.

2. Materials and Methods

2.1. Materials

The titanium dioxide waste acid used in the experiment was prepared by dissolving ferrous sulfate, vanadyl sulfate, magnesium sulfate, manganese sulfate, calcium hydroxide, and aluminum sulfate in deionized water. Composition of titanium dioxide waste acid was shown in Table 1. All the reagents were analytical grade, including hydrogen peroxide and phosphoric acid. The deionized water used in the experiments was produced using a water purification system.

Table 1. Composition of titanium dioxide waste acid [10].

Element	Fe	V	Mg	Mn	Ca	Al
Concentration/g·L ⁻¹	37.64	0.41	5.00	2.15	0.23	1.52

2.2. Experimental Methods

The process of the “step extraction of valuable components from titanium dioxide waste acid” is shown in Figure 1. Our research work is mainly focused on the selective precipitation of iron.

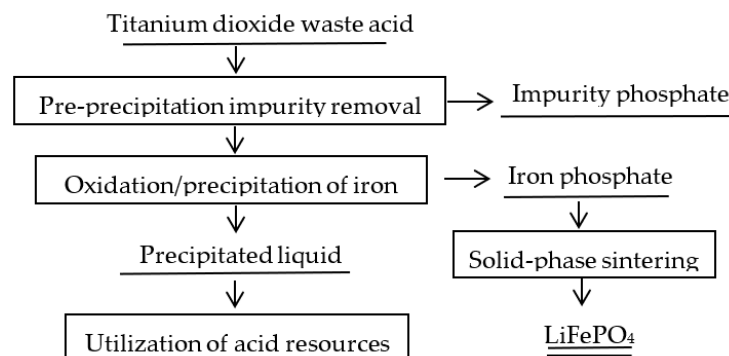


Figure 1. Procedural route for the step extraction of valuable components from titanium dioxide waste acid.

All experiments were performed in a glass beaker with a thermostatic mixing water bath pot. A predetermined amount of titanium dioxide waste acid was added to a beaker

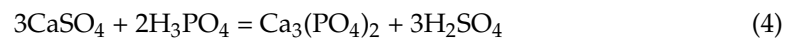
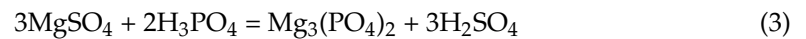
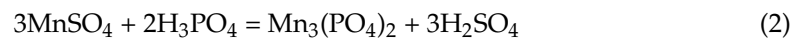
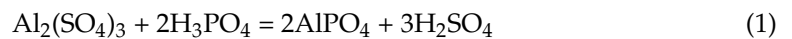
and constantly stirred. Subsequently, the pH value of the solution was adjusted with sulfuric acid and ammonia. The solution was heated to a predetermined temperature.

The experiment was divided into the following two steps.

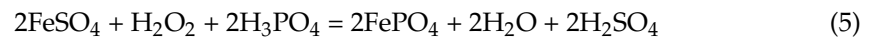
Firstly, by adding a phosphoric acid precipitant in a ferrous reducing state, impurities of aluminum, magnesium, manganese, and calcium react with the precipitant to form a phosphate precipitate, thereby separating and removing impurities.

Then, iron(II) in titanium dioxide waste acid is oxidized by H_2O_2 and is preferentially precipitated with phosphoric acid to form iron(III) phosphate. After the required reaction time has passed, the filtrate is separated from the precipitation through vacuum filtration. The remaining residue is roasted at $700\text{ }^\circ\text{C}$ for 8 h in order to determine the phase of the precipitate [25]. The reaction equation is as follows:

Chemical reaction in the reduced state:



Chemical reaction in the oxidized state:



The experimental conditions for preparing $FePO_4$ under oxidation conditions are as follows: temperature of $60\text{ }^\circ\text{C}$, solution pH = 2.5, reaction time of 25 min, standing period of 1 h, and subsequent filtration. The solid phase is dried and roasted at $700\text{ }^\circ\text{C}$ for 8 h.

2.3. Measurement and Characterization

The crystalline phases of iron phosphate precipitation were detected using XRD (Rigaku, TTR-III). The samples were characterized by scanning electron microscopy (JSM-6360LV, JEOL). Mass fractions of metals in the iron phosphate precipitation were analyzed using an X-ray fluorescence spectrometer (XRF, Rigaku). The particle size distributions of iron phosphate precipitation were measured using a laser particle size meter (Type3000) (Malvern, UK) [26–31].

The purity of the iron phosphate was calculated using the following formula:

$$\theta = \frac{m_{(P_2O_5+Fe_2O_3)}}{m} \times 100\% \quad (6)$$

3. Results and Discussion

3.1. Impurity Removal Experiment in the Reduced State

3.1.1. Thermodynamic Analysis of Impurity Removal via Pre-Precipitation

The solubility product constants of the possible precipitates in the reaction system are listed in Table 2, and the chemical equations, reaction constant data table, and the expansion formulae used in the system are listed in Table 3. Similarly, the following equations were obtained [32–36]:

$$[Fe_{II}] = [Fe^{2+}] + [FeOH^+] + [Fe(OH)_2] + [Fe(OH)_3^-] + [Fe(OH)_4^{2-}] = [Fe^{2+}] + 10^{5.56}[Fe^{2+}][OH^-] + 10^{9.77}[Fe^{2+}][OH^-]^2 + 10^{9.67}[Fe^{2+}][OH^-]^3 + 10^{8.58}[Fe^{2+}][OH^-]^4 \quad (7)$$

$$[P] = C_T = [PO_4^{3-}] + [HPO_4^{2-}] + [H_2PO_4^-] + [H_3PO_4] = [PO_4^{3-}] + 10^{12.36}[H^+][PO_4^{3-}] + 10^{7.2}[H^+][HPO_4^{2-}]/10^{19.57}[H^+][PO_4^{3-}] + 10^{2.04}[H^+][H_2PO_4^-]/10^{21.6}[H^+]^3[PO_4^{3-}] \tag{8}$$

$$[S] = [SO_4^{2-}] + [HSO_4^-] + [H_2SO_4] + [FeSO_4^+] + 2[Fe(SO_4)_2^-] = [SO_4^{2-}] + 10^{1.93}[H^+][SO_4^{2-}] + 10^{-1.07}[H^+][SO_4^{2-}] + 10^{2.03}[Fe^{3+}][SO_4^{2-}] + 2 \times 10^{2.98}[Fe^{3+}][SO_4^{2-}]^2 \tag{9}$$

Table 2. Solubility products of precipitates that may appear in the reaction system (298.15 K).

Substance	State	Solubility Product Constant
Fe ₃ (PO ₄) ₂ ·H ₂ O	solid	K _{sp} = 9.94 × 10 ⁻²⁹
Mn ₃ (PO ₄) ₂ ·nH ₂ O	solid	K _{sp} = 6.13 × 10 ⁻³²
AlPO ₄ ·1.5H ₂ O	solid	K _{sp} = 3.5 × 10 ⁻²¹
Mg ₃ (PO ₄) ₂ ·8H ₂ O	solid	K _{sp} = 6.31 × 10 ⁻²⁶
Fe ₃ (PO ₄) ₂	solid	K _{sp} = 1.3 × 10 ⁻²²
Ca ₃ (PO ₄) ₂	solid	K _{sp} = 2 × 10 ⁻²⁹
Fe(OH) ₃	solid	K _{sp} = 2.79 × 10 ⁻³⁹
Mn(OH) ₂	solid	K _{sp} = 1.9 × 10 ⁻¹³
Al(OH) ₃	solid	K _{sp} = 1.3 × 10 ⁻³³
Mg(OH) ₂	solid	K _{sp} = 5.61 × 10 ⁻¹²
Ca(OH) ₂	solid	K _{sp} = 5.5 × 10 ⁻⁶

Table 3. Chemical equations and their expanded forms in the system.

Equilibrium Reactions	Equilibrium Constants (lgK)	Mathematical Relationships
Fe ³⁺ + OH ⁻ = FeOH ²⁺	11.87	[FeOH ²⁺] = 10 ^{11.87} [Fe ³⁺][OH ⁻]
Fe ³⁺ + 2OH ⁻ = Fe(OH) ₂ ⁺	21.17	[Fe(OH) ₂ ⁺] = 10 ^{21.17} [Fe ³⁺][OH ⁻] ²
Fe ³⁺ + 3OH ⁻ = Fe(OH) ₃	29.67	[Fe(OH) ₃] = 10 ^{29.67} [Fe ³⁺][OH ⁻] ³
Fe ³⁺ + SO ₄ ²⁻ = Fe(SO ₄) ⁺	2.03	[Fe(SO ₄) ⁺] = 10 ^{2.03} [Fe ³⁺][SO ₄ ²⁻]
Fe ³⁺ + 2SO ₄ ²⁻ = Fe(SO ₄) ₂ ⁻	2.98	[Fe(SO ₄) ₂ ⁻] = 10 ^{2.98} [Fe ³⁺][SO ₄ ²⁻] ²
Fe(OH) ₃ = Fe ³⁺ + 3OH ⁻	-38.55	[Fe ³⁺][OH ⁻] ³ = 10 ^{-38.55}
FePO ₄ = Fe ³⁺ + PO ₄ ³⁻	-23	[Fe ²⁺][PO ₄ ³⁻] = 10 ⁻²³

For the orthophosphate of Mx(PO₄)_y, the relationship between [Fe²⁺] and pH is as follows:

$$\lg[Fe^{2+}] = -5.63 + 0.5 \lg(1 + 4.8 \times 10^{21-3pH} + 3.6 \times 10^{19-2pH} + 2.3 \times 10^{12-pH}) \tag{10}$$

For the hydroxides of Fe(OH)₂, the relationship between [Fe²⁺] and pH is as follows:

$$\lg[Fe^{2+}] = 11.69 - 2pH$$

The above two formulas represent the relationship between the molar concentration of the dissolution equilibrium ion and the pH change in Fe₃(PO₄)₂ and Fe(OH)₂, respectively. In the same way, the equilibrium system curve of the molar concentration and the pH values of Mn²⁺, Mg²⁺, Ca²⁺, Al³⁺, Fe²⁺ and other metal ions can be obtained, as shown in Figure 2.

The above two formulas represent the relationship between the equilibrium ion concentration (mol/L) of Fe₃(PO₄)₂ and Fe(OH)₂ in terms of dissolution and pH change, respectively. This indicates that both dissolution and precipitation equilibrium processes change with changes in the pH value and can be used to analyze the precipitation order of various ions in the solution. Similarly, the relationship between the concentration of various metal ions such as Mn²⁺, Mg²⁺, Ca²⁺, Al³⁺, and Fe²⁺ and pH changes can be obtained. The precipitation equilibrium system curve of metal (Mⁿ⁺) ion phosphate and hydroxide is shown in Figure 2.

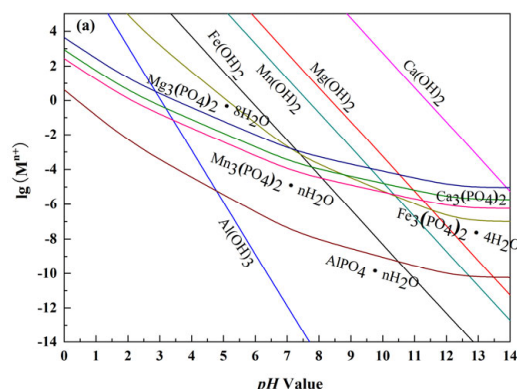


Figure 2. The relationship between $\lg(M^{n+})$ and pH.

According to Figure 2, the precipitation order of orthophosphate is as follows: $\text{AlPO}_4 \cdot 1.5\text{H}_2\text{O}$, $\text{Mg}_3(\text{PO}_4)_2 \cdot 8\text{H}_2\text{O}$, $\text{Ca}_3(\text{PO}_4)_2$, $\text{Mn}_3(\text{PO}_4)_2 \cdot n\text{H}_2\text{O}$, and $\text{Fe}_3(\text{PO}_4)_2$. Furthermore, the precipitation order of hydroxide is as follows: $\text{Al}(\text{OH})_3$, $\text{Fe}(\text{OH})_2$, $\text{Mn}(\text{OH})_2$, $\text{Mg}(\text{OH})_2$, and $\text{Ca}(\text{OH})_2$. From this, it can be inferred that when the concentration of each target element ion in the reactant is determined, the initial pH value of each orthophosphate and hydroxide at the beginning of precipitation can be obtained; that is, by adjusting the pH value, the selective precipitation of each impurity element can be achieved.

The pH values of the critical precipitation of orthophosphate and hydroxide during the reaction process of each ion in this system are shown in Table 4.

Table 4. Critical pH of precipitation of each phosphate and hydroxide in the precipitation reaction system.

Metal Ion	Mn^{2+}	Mg^{2+}	Ca^{2+}	Fe^{2+}	Al^{3+}
$\lg[M^{n+}]$	0.33	0.70	-0.64	1.58	0.18
Initial precipitation pH of orthophosphate	3.07	1.45	3.4	4.1	<0
Initial precipitation pH of hydroxide	7.31	8.04	11.7	5.05	3.0

From Table 4, it can be seen that when $\text{pH} > 0$, in the strongly acidic reaction system, Al^{3+} in the solution already begins to combine with phosphate ions in the solution to induce AlPO_4 precipitation. At the same time, when the reaction system is in the range of $1.45 < \text{pH} < 4$, the orthophosphates of Mn^{2+} , Mg^{2+} , and Ca^{2+} also begin to precipitate. A small amount of $\text{AlPO}_4 \cdot 1.5\text{H}_2\text{O}$, $\text{Mg}_3(\text{PO}_4)_2 \cdot 8\text{H}_2\text{O}$, $\text{Ca}_3(\text{PO}_4)_2$, $\text{Mn}_3(\text{PO}_4)_2 \cdot n\text{H}_2\text{O}$, and $\text{Fe}_3(\text{PO}_4)_2$ are gradually generated in acidic solutions.

According to the above discussion, the content of Al^{3+} , Mn^{2+} , Mg^{2+} , and Ca^{2+} in the reaction system can be adjusted by adjusting the pH during the pre-precipitation process. In the first step, these impurity ions should be settled as much as possible; then, Fe^{2+} should be oxidized to Fe^{3+} ; and, finally, the pH should be adjusted to the best value for one-step precipitation so as to obtain iron phosphate with higher purity in the next step of the precipitation process.

3.1.2. Impurity Removal Experiment

The iron in titanium dioxide waste acid is mainly in the form of ferrous iron. The pH value is adjusted by adding ammonia water, and a phosphoric acid solution with a molar ratio of impurities such as aluminum, magnesium, vanadium, calcium, and manganese is added to it. The temperature is set at 30 °C, the stirring speed is set at 350 r/min, and the reaction time is 20 min.

The XRD pattern of the sample obtained from the initial pre-precipitation is shown in Figure 3. From the figure, it can be seen that when the $\text{pH} = 2.77$, the main precipitation component is AlPO_4 ; when the $\text{pH} = 3.18$, a small portion of Fe precipitates, with AlPO_4 and $\text{Al}_{0.67}\text{Fe}_{0.33}\text{PO}_4$ as the main components; when the $\text{pH} = 4$, the principal components

are basically the same as when the pH = 3.18; and when the pH value of the reaction system solution increases to 5, the precipitation components are Fe_3PO_7 , FePO_4 , $\text{Mn}_2\text{P}_2\text{O}_7$, $\text{Fe}(\text{PO}_3)_3$, and $\text{Al}(\text{PO}_3)_3$, indicating that at this pH, the orthophosphates (metaphosphates) formed by other impurity ions in the solution and some hydroxides gradually begin to precipitate, which provides favorable conditions for the next step of oxidative precipitation to prepare iron phosphate precursors.

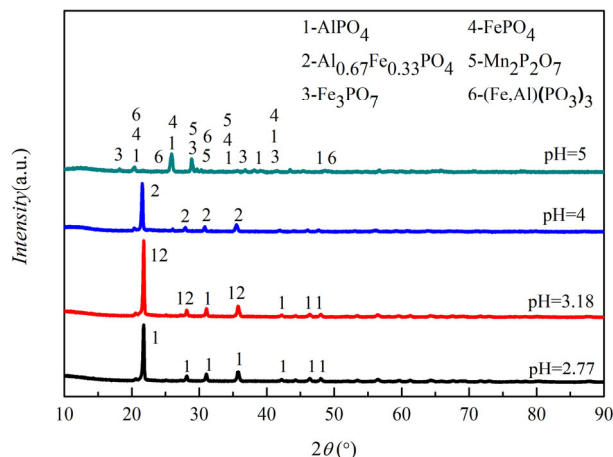


Figure 3. The XRD pattern of the sample obtained from the initial pre-precipitation.

3.2. Study on the Preparation of Iron Phosphate in Oxidized State

3.2.1. The Effect of Temperature on the Product FePO_4

The experimental conditions for the impurity removal process were as follows: in a reduced state, a phosphoric acid solution with an equal molar ratio of the impurity elements aluminum, magnesium, vanadium, calcium, and manganese was added; the pH was set to 3.0, the stirring speed was set to 350 r/min, and the reaction time was set to 20 min; and the effects of impurity removal temperatures of 30 °C, 45 °C, 60 °C, and 75 °C on the final preparation process of iron phosphate were investigated. The experimental conditions for preparing FePO_4 under oxidation conditions were listed in the second experimental section.

The XRD spectra of the samples prepared under different temperatures are shown in Figure 4. In Figure 4a, as the pre-precipitation reaction temperature increases, there is no significant change in the peak strength and peak structure of the final sample, and the main component is iron phosphate. No phosphate precipitation of other impurity metals was found. It can be seen that within this temperature range, the first step of pre-precipitation has a good removal effect on the other impurities.

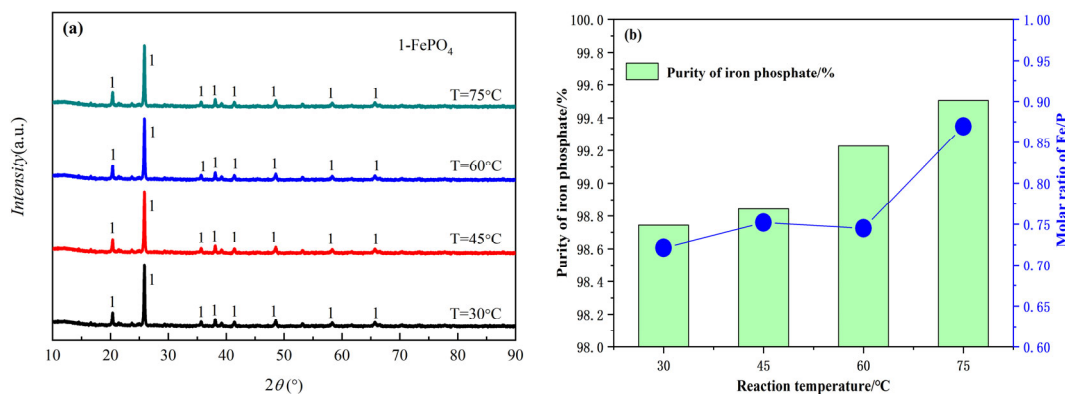


Figure 4. XRD pattern and purity of FePO_4 at different reaction temperatures. ((a) XRD pattern; (b) purity of FePO_4).

The purity of the samples under different temperature systems is shown in Figure 4b, which shows that the purity and the Fe/P molar ratio of the samples increase with the increase in the reaction temperature. As the pre-precipitation temperature increases, the purity of iron phosphate increases from 98.74% at 30 °C to 99.50% at 75 °C. At the same time, the Fe/P molar ratio of the product increases from 0.72 at 30 °C to 0.87 at 75 °C. From these findings, it can be seen that increasing the temperature is beneficial for the removal of other impurities in titanium dioxide waste acid and for improving the purity and Fe/P molar ratio of the iron phosphate produced.

3.2.2. The Effect of Seed Crystals on the Product FePO₄

The experimental conditions for the impurity removal process are as follows: in a reduced state, a phosphoric acid solution with an equal molar ratio of the impurity elements aluminum, magnesium, vanadium, calcium, and manganese was added; the pH was set to 3.0, the stirring speed was set to 350 r/min, the reaction time was set to 20 min, and the temperature was set to 60 °C; and the effects of seed crystals of 0.5 g of FePO₄/50 mL and those of 1.0 g, 1.5 g, and 2.0 g on the final preparation process of iron phosphate were investigated. The experimental conditions for preparing FePO₄ under oxidation conditions were listed in the second experimental section.

The XRD spectra of FePO₄ under different crystal seed addition amounts are shown in Figure 5a. As the number of crystal seeds added increases, the peak strength and peak structure of the final samples do not show significant changes, and the main component is iron phosphate. No phosphate precipitation of other impurity metals was found.

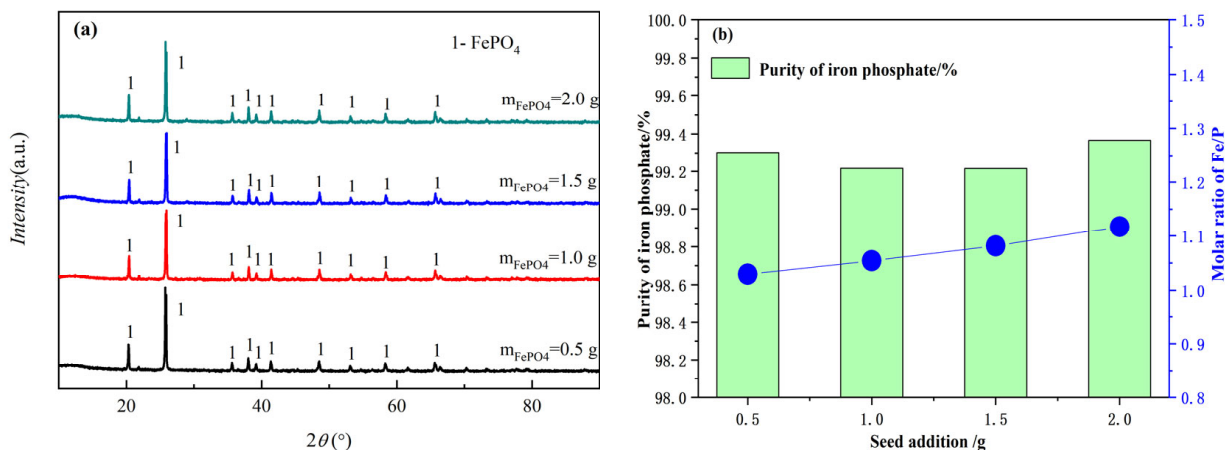


Figure 5. XRD pattern and purity of FePO₄ at different seed addition. ((a) XRD pattern; (b) purity of FePO₄).

The purity and Fe/P molar ratio changes of the samples under different crystal seed addition amounts are shown in Figure 5b. With the increase in seed addition, the purity of the sample remained almost unchanged (99.30~99.37%), and the Fe/P molar ratio slightly increased from 1.02 to 1.17. This is consistent with the XRD results shown in Figure 5a; that is, the number of crystal seeds added within this range has almost no effect on the phase, purity, and Fe/P molar ratio in the iron(III) phosphate precipitation process.

3.2.3. The Effect of pH on the Produced FePO₄

The experimental conditions for the impurity removal process are as follows: in a reduced state, a phosphoric acid solution with an equal molar ratio of the impurity elements aluminum, magnesium, vanadium, calcium, and manganese was added; the pH was set to 3.0, the stirring speed was set to 350 r/min, the reaction time was set to 20 min, and the temperature was set to 60 °C; and the effects of the pH values of 3.0, 3.5, 4.0, 4.5, and 5.0 on the final preparation process of iron phosphate were investigated. The experimental

conditions for preparing FePO_4 under oxidation conditions were listed in the second experimental section.

The XRD spectra of the samples prepared under different pH conditions are shown in Figure 6a. Phase analysis showed that the main component was FePO_4 , and the crystal form of the sample was hexagonal. In the pH range (3.0–4.5) investigated, the position of the generated XRD characteristic peak of Iron(III) phosphate basically remained unchanged, but the intensity of the characteristic peak increased with the increase in pH (3.0–3.5). As the pH value (3.5–5.0) was progressively increased, the characteristic peak intensity decreased. When the pH was too high, the peak strength of the sample showed signs of weakening, so the pH of the reaction system should not be too high.

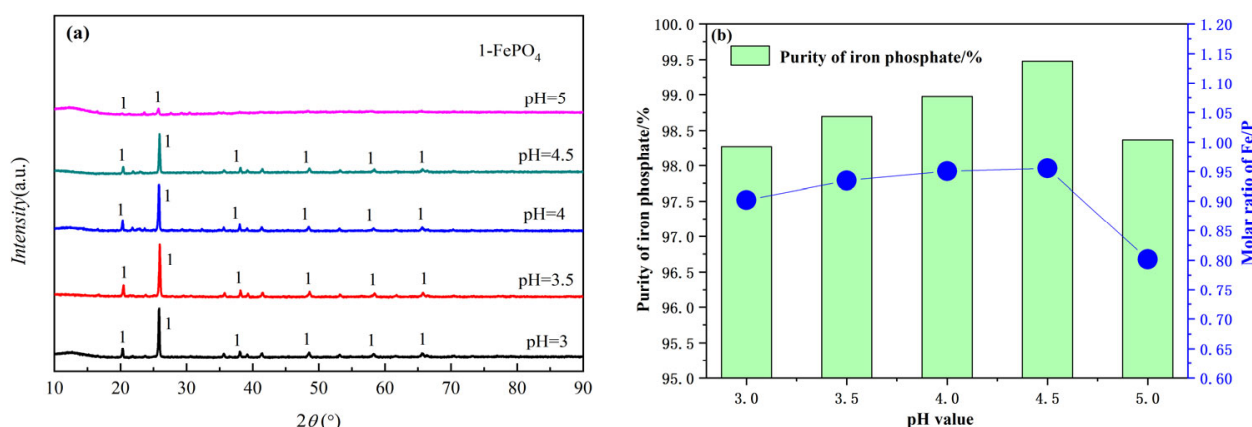


Figure 6. XRD pattern and purity of FePO_4 at different pH. ((a) XRD pattern; (b) purity of FePO_4).

The purity and Fe/P molar ratio of the samples prepared at different pH values of the solution are shown in Figure 6b. As the pH value increased from 3.0 to 4.5, the purity of the sample increased from 98.27% to 99.48%, and the Fe/P ratio of the sample increased from 0.90 to 0.95. As the pH value continued to increase to 5.0, the sample purity and Fe/P ratio decreased to 98.36% and 0.80, respectively, which is a finding that is consistent with the thermodynamic analysis results and XRD results. That is to say, as the pH increases from 3.0 to 4.5, the phase strength, purity, and Fe/P ratio of the precipitate correspondingly increase. When continuing to increase the pH to 5.0, these values will actually decrease.

3.2.4. The Effect of P/M on the Product FePO_4

The experimental conditions for the impurity removal process are as follows: in a reduced state, a phosphoric acid solution with an equal molar ratio of the impurity elements aluminum, magnesium, vanadium, calcium, and manganese was added; the pH was set to 3.0, the stirring speed was set to 350 r/min, the reaction time was set to 20 min, and the temperature was set to 60 °C; and the effects of P/M 1.0, 1.1, 1.1, 1.2, 1.3, and 1.4 on the final preparation process of iron phosphate were investigated. The experimental conditions for preparing FePO_4 under oxidation conditions were listed in the second experimental section.

The XRD spectra of the samples prepared under different $\text{H}_3\text{PO}_4/\text{M}^{n+}$ molar ratios are shown in Figure 7a. With the increase in the $\text{H}_3\text{PO}_4/\text{M}^{n+}$ molar ratio in the first step of the pre-precipitation system, the peak structure of the prepared samples did not change significantly, and the peak intensity weakened accordingly, with the main component being hexagonal FePO_4 .

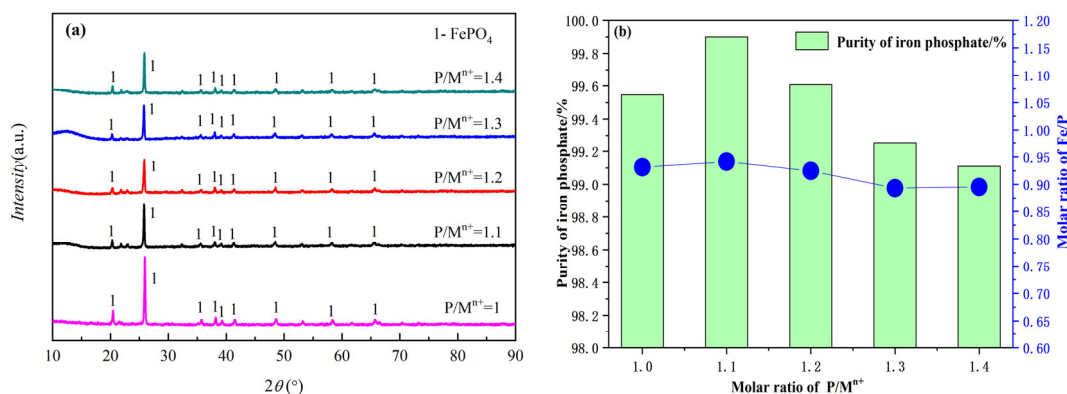


Figure 7. XRD pattern and purity of FePO₄ at different molar ratio of H₃PO₄/Mⁿ⁺. ((a) XRD pattern; (b) purity of FePO₄).

The purity and Fe/P molar ratios of the samples prepared under different molar ratios of H₃PO₄/Mⁿ⁺ are shown in the Figure 7b. As the molar ratio of H₃PO₄/Mⁿ⁺ increases from 1.0 to 1.1, the purity of the sample increases from 99.54% to 99.90%, and the Fe/P molar ratio of the sample increases from 0.93 to 0.94. As the molar ratio of H₃PO₄/Mⁿ⁺ continues to increase to 1.4, the sample purity and Fe/P ratio decrease to 99.11% and 0.90, respectively. It can be concluded that a molar ratio of 1.1 is more suitable for H₃PO₄/Mⁿ⁺. The purity and Fe/P molar ratio of the sample is consistent with the XRD results. That is to say, as the P/M molar ratio increases from 1.0 to 1.1, the phase strength, purity, and Fe/P ratio of the precipitate correspondingly increase. When continuing to increase the P/M molar ratio to 1.4, these values will actually decrease.

3.3. TG-DSC Analysis and Chemical Composition Analysis of Iron Phosphate

The TG–DSC curve of the sample is shown in Figure 8, and by converting the weight loss rate, $x = 2.095$ in FePO₄ · x H₂O was obtained. Excluding errors, the type of iron phosphate prepared in the experiment was FePO₄ · 2H₂O.

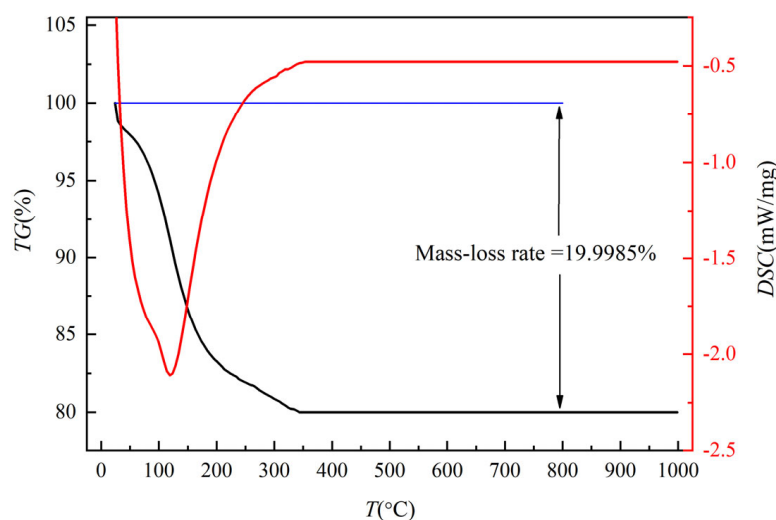


Figure 8. TG-DSC curve of FePO₄.

The indicators of the comparison between the prepared iron phosphate and product standards are shown in Table 5; most of the indicators of the prepared iron phosphate meet the product standards, but there are still some indicators that have a small gap with respect to the product standards.

Table 5. Comparison of indicators between prepared iron phosphate and product standards.

Component/wt. %	Fe	P	Fe/P Ratio	H ₂ O	Ca	Mg	Na/K	Cu/Zn/Ni	Sulfate	D50, μm
Experiment products	28.24	17.52	0.89	19.38	0	0.024	/	/	0.0065	16.81
Technical indicators (standards)	29.0~30.0	16.2~17.2	0.97~1.02	19.0~21.0	<0.005	<0.005	<0.01	<0.005	<0.01	2~6

4. Conclusions

Our research team proposed a new technique consisting of step extraction and the comprehensive utilization of titanium dioxide waste acid. In this paper, the thermodynamics of selective precipitation and the preparation of doped iron phosphate from waste acid were studied. The thermodynamics of impurity removal via pre-precipitation and the effects of reaction temperature, the addition of seed crystals, pH value, and P/M on the precipitation process were investigated in detail. The findings are as follows:

- (1) The effect of reaction temperature, seed crystals, pH value, and P/M on the precipitation process were investigated in detail. The experimental results show that in the reduced state, the optimal precipitation condition is a temperature of 75 °C, an initial pH value of 4.5, and an optimal P/M molar ratio of 1.1.
- (2) The thermodynamics results show that the content of Al³⁺, Mn²⁺, Mg²⁺, and Ca²⁺ in the reaction system can be adjusted by adjusting the pH during the pre-precipitation process. In the first step, these impurity ions should be settled as much as possible; then, Fe²⁺ should be oxidized to Fe³⁺ so as to obtain iron phosphate with higher purity in the next step of the precipitation process.
- (3) In the oxidized state, the following ideal conditions were determined: a temperature of 60 °C, a solution pH = 2.5, and a reaction time of 25 min. After calcination, the precipitate mainly consisted of iron phosphate, which basically meets the requirements of an iron phosphate precursor.

Author Contributions: X.C.: data curation, funding acquisition, and resources; Y.C.: investigation, original draft preparation; X.L.: methodology; Y.L.: review and editing; W.Z.: methodology, supervision; Z.C.: review and editing; T.Z.: software. All authors have read and agreed to the published version of the manuscript.

Funding: This research was supported by the National Natural Science Foundation of China (No. 52204358).

Institutional Review Board Statement: Not applicable.

Informed Consent Statement: Not applicable.

Data Availability Statement: Not applicable.

Acknowledgments: This research was supported by the National Natural Science Foundation of China (52204358); the Guangxi Science and Technology Base and Talent Special (Guike AD 22035105); and the Open foundation of state environmental protection key laboratory of mineral metallurgical resources utilization and pollution control (HB202105).

Conflicts of Interest: The authors declare that they have no known competing financial interests or personal relationships that could have appeared to influence the work reported in this paper.

References

1. Pei, R. *Production of Titanium Dioxide by Sulfuric Acid Method*; Chemical Industry Press: Beijing, China, 1982; pp. 272–275. (In Chinese)
2. Xu, H.; Fu, M. Research process in comprehensive utilization of spent acid and waste water in titanium dioxide production. *Multipurp. Util. Miner. Resour.* **2006**, *4*, 34–37. (In Chinese)
3. Li, L. Research Progress on Comprehensive Recycle of Waste Acid in Titanium Pigment Production at Home and Abroad. *Hydrometall. China* **2010**, *29*, 150–155. (In Chinese)

4. Zhao, Y.; Zhang, Y.; Xing, W.; Xu, N. Treatment of titanium white waste acid using ceramic microfiltration membrane. *Chem. Eng. J.* **2005**, *111*, 31–38. [[CrossRef](#)]
5. Feng, X.; Jiang, L.; Song, Y. Titanium white sulfuric acid concentration by direct contact membrane distillation. *Chem. Eng. J.* **2016**, *285*, 101–111. [[CrossRef](#)]
6. Xu, T.; Yang, W. Sulfuric acid recovery from titanium white (pigment) waste liquor using diffusion dialysis with a new series of anion exchange membranes—Static runs. *J. Membr. Sci.* **2001**, *183*, 193–200.
7. Zhang, T.; Lv, G.; Liu, Y.; Zhang, G. A Comprehensive Utilization Method of Titanium White Waste Acid. CN Patent 104178632 B, 22 June 2016.
8. Zhang, T.; Zhang, W.; Lv, G.; Dou, Z.; Liu, Y. A Method of Treating Titanium White Waste Acid by Steel Slag. CN Patent 201810288264.X, 10 July 2018.
9. Zhang, T.; Lv, G.; Dou, Z.; Liu, Y.; Zhang, W. A Method of Treating Titanium White Waste Acid with Steel Slag and Extracting Valuable Components. CN Patent 201810296696.5, 7 September 2018.
10. Zhang, W.; Zhang, T.; Lv, G.; Zhou, W. Extraction Separation of Sc(III) and Fe(III) from a Strongly Acidic and Highly Concentrated Ferric Solution by D2EHPA/TBP. *JOM* **2018**, *70*, 2837–2845. [[CrossRef](#)]
11. Zhang, Y.; Zhang, T.; Dreisinger, D.; Lv, C.; Lv, G.; Zhang, W. Recovery of vanadium from calcification roasted-acid leaching tailing by enhanced acid leaching. *J. Hazard. Mater.* **2019**, *369*, 632–641. [[CrossRef](#)]
12. Zhang, G.; Zhang, T.; Zhang, Y.; Lv, G.; Liu, Y.; Liu, Z. Pressure leaching of converter vanadium slag with waste titanium dioxide. *Rare Met.* **2016**, *35*, 576–580. [[CrossRef](#)]
13. Wu, L.; Li, X.; Wang, Z. A novel process for producing synthetic rutile and LiFePO_4 cathode material from ilmenite. *J. Alloys Compd.* **2010**, *506*, 271–278. [[CrossRef](#)]
14. Wu, L.; Li, X.; Wang, Z. Preparation of synthetic rutile and metal-doped LiFePO_4 from ilmenite. *Powder Technol.* **2010**, *199*, 293–297. [[CrossRef](#)]
15. Fan, Q.; Lei, L.; Xu, X. Direct growth of FePO_4 /graphene and LiFePO_4 /graphene hybrids for high rate Li-ion batteries. *J. Power Sources* **2014**, *257*, 65–69. [[CrossRef](#)]
16. Prosini, P.; Lisi, M.; Scaccia, S. Synthesis and characterization of amorphous hydrated FePO_4 and its electrode performance in lithium batteries. *J. Electrochem. Soc.* **2002**, *149*, A297–A301. [[CrossRef](#)]
17. Liu, H. Synthesis of nanorods FePO_4 via a facile route. *J. Nanopart. Res.* **2010**, *12*, 2003–2006. [[CrossRef](#)]
18. Kahoul, A.; Hammouche, A. Electrochemical performances of FePO_4 -positive active mass prepared through a new sol-gel method. *Ionics* **2010**, *16*, 105–109. [[CrossRef](#)]
19. Wu, Y.; Chen, L.; Xie, K. Synthesis and characterization of multi-wall carbon nanotubes supported-hydrated iron phosphate cathode material for lithium-ion cells by a novel homogeneous precipitation method. *Ionics* **2012**, *18*, 721–729. [[CrossRef](#)]
20. Wang, Y.; Chen, F.; Ma, X.; Zhang, G. Recovery of nitric and acetic acids from etching waste solution using a synergistic system of N235 and TRPO in cyclohexane. *Hydrometallurgy* **2019**, *185*, 23–29. [[CrossRef](#)]
21. Chen, F.; Wang, X.; Liu, W. Selective extraction of nitric and acetic acids from etching waste acid using N235 and MIBK mixtures. *Sep. Purif. Technol.* **2016**, *169*, 50–58. [[CrossRef](#)]
22. Li, C.; Li, G.; Guo, H. Synthesis of FePO_4 by electrolyzing ferrophosphorus. *Phosphate Compd. Fertil.* **2014**, *29*, 13–15. (In Chinese)
23. Yang, J.; Lv, N.; Su, C. Research progress on the recycling of phosphorus resource from converter steelmaking slag. *Appl. Chem. Ind.* **2019**, *48*, 1440–1446. (In Chinese)
24. Li, H.; Xing, S.; Liu, Y. Recovery of Lithium, Iron, and Phosphorus from Spent LiFePO_4 Batteries Using Stoichiometric Sulfuric Acid Leaching System. *Acs Sustain. Chem. Eng.* **2017**, *5*, 8017–8024. [[CrossRef](#)]
25. Zhang, W.; Zhang, T.; Cai, L. Preparation of Doped Iron Phosphate by Selective Precipitation of Iron from Titanium Dioxide Waste Acid. *Metals* **2020**, *10*, 789. [[CrossRef](#)]
26. Lu, Y.; Xu, Y.; Yang, B. A versatile method for preparing FePO_4 as a promising electrode material rechargeable lithium batteries. *J. Lanzhou Univ. (Nat. Sci.)* **2007**, *43*, 144–146.
27. Guo, X.; Ding, W.; Chen, H. Preparation and characterization of nanosized Fe-P-O catalyst. *J. Fuel Chem. Technol.* **2000**, *28*, 385–387.
28. Son, D.; Kim, E.; Kim, T. Nanoparticle iron-phosphate anode material for Li-ion battery. *Appl. Phys. Lett.* **2004**, *85*, 5875–5877. [[CrossRef](#)]
29. Guo, X.; Ding, W.; Wang, X. Synthesis of a novel mesoporous iron phosphate. *Chem. Commun.* **2001**, *8*, 709–710. [[CrossRef](#)]
30. Zaghba, K.; Julien, C. Structure and electrochemistry of $\text{FePO}_4 \cdot 2\text{H}_2\text{O}$ hydrate. *Power Sources* **2005**, *142*, 279–284. [[CrossRef](#)]
31. Song, Y.; Zavalij, P.; Suzuki, M. New Iron(III) Phosphate: Crystal structure and electrochemical and magnetic properties. *Inorg. Chem.* **2002**, *41*, 5778–5786. [[CrossRef](#)]
32. Speight, J.G. *Lange's Handbook of Chemistry*; McGraw-Hill: New York, NY, USA, 2004.
33. Xiao, C.; Xiao, L.; Gao, C. Thermodynamic study on removal of magnesium from lithium chloride solutions using phosphate precipitation method. *Sep. Purif. Technol.* **2015**, *156*, 582–587. [[CrossRef](#)]
34. He, L.; Xu, W.; Song, Y.; Liu, X.; Zhao, Z. Selective removal of magnesium from a lithium-concentrated anolyte by magnesium ammonium phosphate precipitation. *Sep. Purif. Technol.* **2017**, *187*, 214–220. [[CrossRef](#)]

35. Xiao, C.; Zeng, L.; Wei, J.; Xiao, L.; Zhang, G. Thermodynamic analysis for the separation of tungsten and aluminium in alkaline medium using solvent extraction. *Hydrometallurgy* **2017**, *174*, 91–96. [[CrossRef](#)]
36. Zhang, W.; Zhang, T.; Lv, G. Thermodynamic study on the V(V)-P(V)-H₂O system in acidic leaching solution of vanadium-bearing converter slag. *Sep. Purif. Technol.* **2019**, *218*, 164–172. [[CrossRef](#)]

Disclaimer/Publisher's Note: The statements, opinions and data contained in all publications are solely those of the individual author(s) and contributor(s) and not of MDPI and/or the editor(s). MDPI and/or the editor(s) disclaim responsibility for any injury to people or property resulting from any ideas, methods, instructions or products referred to in the content.